Computers and Electronics in Agriculture 191 (2021) 106565

Contents lists available at ScienceDirect

Computers and Electronics in Agriculture

journal homepage: www.elsevier.com/locate/compag

LiDAR-sensed tree canopy correction in uneven terrain conditions using a sensor fusion approach for precision sprayers

Md Sultan Mahmud [a,b], Azlan Zahid [c], Long He [a,b,*], Daeun Choi [a], Grzegorz Krawczyk [b,d], Heping Zhu [e]

[a] Department of Agricultural and Biological Engineering, The Pennsylvania State University, University Park, PA, USA
[b] Fruit Research and Extension Center, The Pennsylvania State University, Biglerville, PA, USA
[c] Texas A&M AgriLife Research, Texas A&M University System, Dallas, TX, USA
[d] Department of Entomology, The Pennsylvania State University, University Park, PA, USA
[e] Application Technology Research Unit, Agricultural Research Service, U.S. Department of Agriculture, Wooster, OH, USA

ARTICLE INFO

Keywords:
Orchard sprayer
Precision spraying
Canopy density
Sensor fusion
Terrain monitoring

ABSTRACT

Precision spraying is one of the most promising techniques to produce healthy and sustainably profitable crops. However, accurate canopy density measurements for precision spraying decisions are still a challenging endeavor, especially in orchards with uneven terrain conditions. A sensor fusion-based canopy point correction system was developed with a 3D light detection and ranging (LiDAR) sensor and an inertial navigation system-global navigation satellite system (INS-GNSS) for accurate tree canopy density measurement. The LiDAR sensor was used to acquire the tree canopy architectures, while the INS-GNSS sensor was to evaluate the terrain slopes and the tree georeferenced locations. A mathematical model was developed to perform the simulation for correction of canopy points based on given changes in the roll, pitch, and yaw angles. A sensor fusion algorithm was developed to process the canopy point corrections for the tree fruit orchards with three different sloping conditions, including longitudinal, lateral, and combination of both slopes. Simulation results reported that the developed model established the correction of tree canopy points with varying roll, pitch, and yaw angles. Field evaluation results suggested that the developed system could be used for correcting canopy points at any sloping conditions in various terrains. The measured tree canopy density from the corrected canopy points reported a possible of off-target chemical reduction up to 13.87%, 5.19%, and 15.45% in orchard sites 1, 2 and 3, respectively. With the accurate tree canopy density measurement, it is anticipated that the developed system could be used to reduce the off-target deposition for precision spraying applications in uneven tree fruit orchards.

1. Introduction

Characterization of fruit tree architecture such as canopy density and volume is important for applying the correct amount of agrochemicals to prevent overdosing or underdosing target trees. Overdose wastes a significant amount of chemicals, potentially increase production costs, and raises the risk of environmental contamination. Underdose may result in inadequate disease and pest protection triggering crop yield losses. Inappropriate chemical applications cause about $8.2 billion annual environmental and economic losses in the United States (Pimentel & Burgess, 2014). Target-oriented variable-rate spraying, also called precision spraying, is an effective method to apply agrochemicals. The characteristic information of targets adjusts the spraying parameters to support variable-rate spraying tasks and improve droplet deposition and coverage (Miranda-Fuentes et al., 2015; Song et al., 2015). Thus, accurate measurement of tree characteristics is of utmost importance.

Tree canopy density is one of the vital target characteristics used to adjust the nozzle and airflow rates to apply the spray to targeted spots and reduce drift (Landers, 2011; Landers, 2010). It characterizes tree structure and helps determine the appropriate spray rate for precision agrochemical applications (Chen, Zhu, & Ozkan, 2012; Hu & Whitty, 2019). Various sensing techniques have been tested for tree canopy characteristics measurements, including digital photographic, ultrasonic, spectral, infrared, and laser (Asaei, Jafari, & Loghavi, 2019; Chen et al., 2019; Gil et al., 2007; He et al., 2011). Although significant efforts have been made to determine tree canopy characteristics using various

* Corresponding author.
E-mail address: luh378@psu.edu (L. He).

https://doi.org/10.1016/j.compag.2021.106565
Received 9 August 2021; Received in revised form 18 October 2021; Accepted 9 November 2021
Available online 18 November 2021
0168-1699/© 2021 Elsevier B.V. All rights reserved.

sensors, challenges still exist in measuring canopy density in real-time field conditions due to uncontrollable environmental conditions and sensor limitations. The digital photographic technique is highly affected by illumination variations, wind speed, and system vibrations which can reduce the performance of the system (Asaei, Jafari, & Loghavi, 2019). Ultrasonic sensors are also affected by outdoor environmental conditions and provide inaccurate sensing data due to the large angle of divergence of ultrasonic waves (Zhang et al., 2018). Consequently, spectral and infrared sensors show inferior performance due to high sensitivity to illumination variations and uncontrollable weather conditions (Zhang et al., 2018). Conversely, laser sensors are independent of outdoor field conditions and provide more accurate canopy structures under different environmental conditions (Liu & Zhu, 2016).

LiDAR (light detection and ranging) sensing is a breakthrough remote sensing technology using laser light analogous to radar, which directly measures tree canopy characteristics (Hosoi & Omasa, 2006; Omasa, Hosoi, & Konishi, 2007). The LiDAR sensor measures the roundtrip time for a pulse of laser energy to travel between the sensor and target. The incident of the pulse of energy bounces off vegetation canopy, branches, and trunk surfaces, then back to the instrument, enabling exterior structure and three-dimensional information of the tree through a receiver. Applications of LiDAR-based laser sensors have been investigated in tree canopy characterizations (Liu & Zhu, 2016; Shalal et al., 2015; Zeng, Feng, & He, 2020). Liu and Zhu (2016) used a 2D laser scanning system to detect complex shape structures of individual trees and confirmed the capability for accurate tree canopy characterization in real-time orchard conditions. Shalal et al. (2015) achieved about 96.64% accuracy while detecting apple tree trunks using a 3D laser sensor and reported that the sensor was able to provide reliable angles and width of the tree trunks and non-tree objects information. The 3D LiDAR sensor was also used in segmenting geometric characteristics and obstacles in the apple orchard, including the trellis wires, support poles, and tree trunks with detection accuracies of 88.6%, 82.1%, and 94.7%, respectively (Zeng, Feng, & He, 2020). Apart from the geometric characterization, LiDAR sensors for calculating tree canopy foliage density measurement have also been reported (Berk et al., 2020; Chakraborty et al., 2019; Hu & Whitty, 2019).

The aforementioned studies were mainly conducted in certain regions with flat terrain, while fruit orchards in Pennsylvania are typically located on uneven terrains with variable slopes. The rough terrain conditions can cause deviations of the angular orientation of the LiDAR sensor during tree canopy scanning, which may result in the positioning error of the sensing data (Palleja et al., 2010). Inaccurately measured canopy data could result in erroneous tree canopy density, which directly contributes to the off-target deposition of spray droplets during spraying operations. Excessive off-target deposition can occur in places where the terrain slope changes suddenly and greatly. In a sprayer, the LiDAR sensor and nozzles are typically mounted separately at different locations with a certain distance between them. The difference in the sensing and nozzle positions when traveling on a sloped path is illustrated in Fig. 1. After the sensor scans the tree at a given position, the sprayer moves forward to spray the tree based on the sensing decision. However, with a slope change, the positioning difference misguides the nozzles to spray at the wrong position and miss the target.

Palleja et al. (2010) revealed that the positioning error of the LiDAR sensor could be corrected by using positioning sensors such as inertial measurement units (IMU) in different sloping conditions. An IMU sensor is an electronic sensor that uses accelerometers and gyroscopes to measure acceleration and rotation, which can be used to measure the movement of an object (i.e., canopy sensing system in our case) based on the roll, pitch, and yaw angles. These are the three rotational movements when an object moves through a medium. Roll describes the position change in the x-axis based on side slope (lateral slope), pitch describes the change in y-axis based on uphill or downhill (longitudinal slope), and yaw describes the change in the z-axis/heading direction. Although significant advancements in automated technologies for agricultural applications have been made in the last decade, very few studies have been reported for LiDAR sensed tree canopy position corrections, particularly for precision spraying. Most of the previous studies aimed only to correct the acquired point clouds but did not consider correcting tree canopy points for accurate canopy density measurements and off-target deposition calculations.

The primary goal of this study was to measure accurate tree canopy density and possible off-target deposition by solving the positioning error problem for precision spraying systems where slope change occurs by integrating LiDAR and INS-GNSS sensors with a sensor fusion approach. The specific objectives were to (1) simulate the position changes of the tree canopy points based on the roll, pitch, and yaw angles, (2) correct the tree canopy positions in three different slopes, including longitudinal, lateral, and combination of longitudinal and lateral slopes in the orchard environment, and (3) evaluate the canopy density change due to slope variation and calculate possible off-target deposition.

2. Materials and methods

2.1. Concept of canopy corrections

The relative position displacement of the tree canopy to the sprayer system varies due to the change of the ground slopes. According to

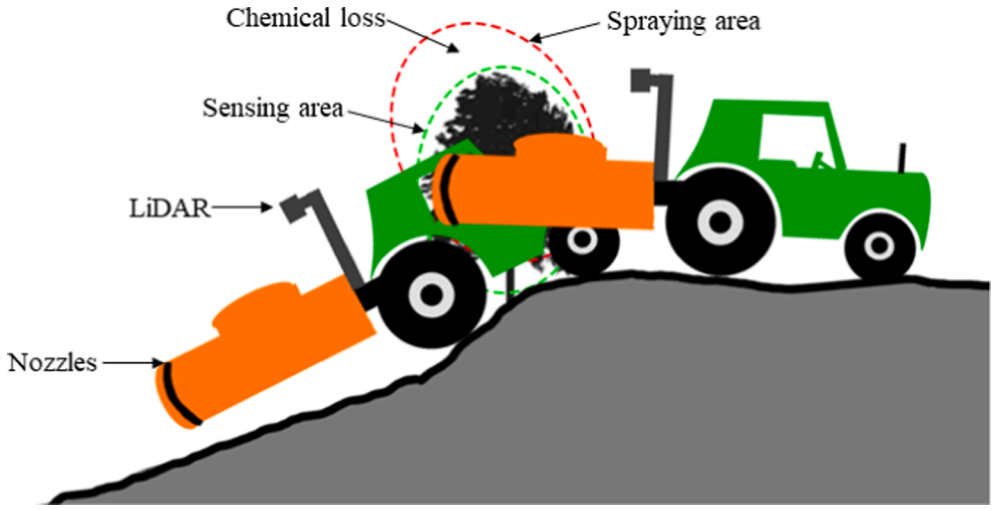

Fig. 1. Illustration of sensing and spraying position variations in slope change.

Euler's theorem, any rotation of a 3D object can be described by three Euler angles (e.g., roll, pitch, and yaw). The roll is the longitudinal axis, and the pitch is the lateral axis, and the yaw is the vertical axis (Fig. 2). For a sprayer, the roll axis runs through the body of the sprayer from back to front in the direction of travel; the pitch axis runs from the side left to right and perpendicular to the direction of travel along the horizontal plane; and the yaw axis is drawn from top to bottom and perpendicular to the roll and pitch axis along the vertical plane.

Three types of slopes are usually found in Pennsylvania fruit orchards, including longitudinal, lateral, and combination of longitudinal and lateral slopes (Fig. 3). The longitudinal represents the slope that is parallel to the sprayer driving direction, while the lateral indicates the slope that is perpendicular to the driving direction of the sprayer. The change of the ground slopes can be described by the changes in navigating a sprayer body posture (roll, pitch, and yaw). The variation of the longitudinal slope can be described by the change in pitch angle, that of the lateral slope can be described by the change of roll angle, and that of the combination of both slopes can be described by the change in roll and pitch together. The yaw describes the sprayer rotation around the vertical axis.

An illustration of the Euler angle changes of acquired point cloud data by a LiDAR sensor and the corresponding correction is presented in Fig. 2. The mathematical model (H) was developed using the rotation matrices and position matrix (Eq. (1)). The rotation matrix is a matrix that is used to perform a rotation in Euclidean space. The position matrix defines the original position of the point in the x, y, and z-axis. All matrices were scaled to 4 × 4 for conversion to the form of the transformation matrix. The matrices multiplication sequence in the model followed the widely adopted convention, which implies that the rotation order was z, y, and the x-axis. The resultant equation (Eq. (2)) of matrix multiplication has two components, including rotation and translation. The rotational component (first 3 × 3 matrix) provides the orientation/direction of position change, and the translational component (first three elements of column 4) gives the corrected position coordinate of the tree point cloud, based on the roll, pitch, and yaw angles. The corrected positions of the point in x, y, and z-axis were calculated using Eq. (3), 4, and 5, respectively.

$$H = R_z(\theta_w)R_y(\theta_P)R_x(\theta_r)P_0 \tag{1}$$

$$= \begin{bmatrix} \cos\theta_w & -\sin\theta_w & 0 & 0 \\ \sin\theta_w & \cos\theta_w & 0 & 0 \\ 0 & 0 & 1 & 0 \\ 0 & 0 & 0 & 1 \end{bmatrix} \begin{bmatrix} \cos\theta_P & 0 & \sin\theta_P & 0 \\ 0 & 1 & 0 & 0 \\ -\sin\theta_P & 0 & \cos\theta_P & 0 \\ 0 & 0 & 0 & 1 \end{bmatrix} \begin{bmatrix} 1 & 0 & 0 & 0 \\ 0 & \cos\theta_r & -\sin\theta_r & 0 \\ 0 & \sin\theta_r & \cos\theta_r & 0 \\ 0 & 0 & 0 & 1 \end{bmatrix} \begin{bmatrix} 1 & 0 & 0 & x \\ 0 & 1 & 0 & y \\ 0 & 0 & 1 & z \\ 0 & 0 & 0 & 1 \end{bmatrix}$$

$$= \begin{bmatrix} \cos\theta_p\cos\theta_w & -\cos\theta_p\sin\theta_w & \sin\theta_p & \cos\theta_p(\sigma_3) + z\sin\theta_p \\ \cos\theta_r\sin\theta_w + \cos\theta_w\sin\theta_p\sin\theta_r & \cos\theta_r\cos\theta_w - \sin\theta_p\sin\theta_r\sin\theta_w & -\cos\theta_p\sin\theta_r & \cos\theta_r(\sigma_1) + \sin\theta_r(\sigma_2) \\ \sin\theta_r\sin\theta_w - \cos\theta_r\cos\theta_w\sin\theta_p & \cos\theta_w\sin\theta_r + \cos\theta_r\sin\theta_p\sin\theta_w & \cos\theta_p\sin\theta_r & \sin\theta_r(\sigma_1) - \cos\theta_r(\sigma_2) \\ 0 & 0 & 0 & 1 \end{bmatrix} \tag{2}$$

where

$$\sigma_1 = y\cos\theta_w + x\sin\theta_w$$

$$\sigma_2 = \sin\theta_p\sigma_3 - z\cos\theta_p$$

$$\sigma_3 = x\cos\theta_w - y\sin\theta_w$$

The coordinates of the corrected position at x, y, and z-axis can be described as:

$$\mathbf{P_{C,x}} = \cos(\theta_P) \times \{x\cos(\theta_w) - y\sin(\theta_w)\} + z\sin(\theta_P) \tag{3}$$

$$\mathbf{P_{C,y}} = \cos(\theta_r) \times \{y\cos(\theta_w) + x\sin(\theta_w)\} + \sin(\theta_r) \times [\sin(\theta_P) \times \{x\cos(\theta_w) - y\sin(\theta_w)\} - z\cos(\theta_P)] \tag{4}$$

$$\mathbf{P_{C,z}} = \sin(\theta_r) \times \{y\cos(\theta_w) + x\sin(\theta_w)\} - \cos(\theta_r) \times [\sin(\theta_P) \times \{x\cos(\theta_w) - y\sin(\theta_w)\} - z\cos(\theta_P)] \tag{5}$$

where R_x, R_y, and R_z are the rotation matrices around x, y, and z-axis; P_0 is the position matrix which gives the x, y, and z coordinate of the tree canopy point; θ_r, θ_P, and θ_w are the change in roll, pitch and yaw angles, respectively, and $P_{C,x}$, $P_{C,y}$, and $P_{C,z}$ are the corrected positions in the x, y, and z-axis directions, respectively.

Prior to field testing, a simulation was performed to derive the correction equations for position changes in x, y, and z-axis directions to correct the tree canopy position. The simulations were performed using MATLAB® software (The MathWorks Inc, Natick, MA, USA). Different input parameters, including angle changes of the roll, pitch, and yaw, were used to evaluate the performance of the developed model. The effects of 20° of roll angle, 20° of pitch angle, and 20° of both roll and pitch angle changes were investigated for the evaluation of tree canopy point correction. The effect of yaw angle change was not considered in the simulation because the change in angle is minor/negligible when the sprayer is traveling straight in the orchard rows. The corrected positions were plotted in a 3D graph to visualize the differences caused by the roll, pitch, and both angle changes for the given tree canopy points.

2.2. Sensor system integration

An integrated sensor system comprised of a 3D VLP-16 LiDAR scanner (Velodyne LiDAR, San Jose, CA, USA), an Inertial Navigation System-Global Navigation Satellite System (INS-GNSS) (Inertial Labs, Paeonian Springs, VA, USA), and two laptop computers (Dell, Round Rock, TX, USA) with an Intel® i7-9750 central processing unit (CPU) running at 2.6 Gigahertz (GHz), 16 Gigabyte (GB) of Random Access Memory (RAM) (Fig. 4). The system was mounted on to a utility vehicle (Kubota, Osaka, Japan) that drives through the apple orchard row for

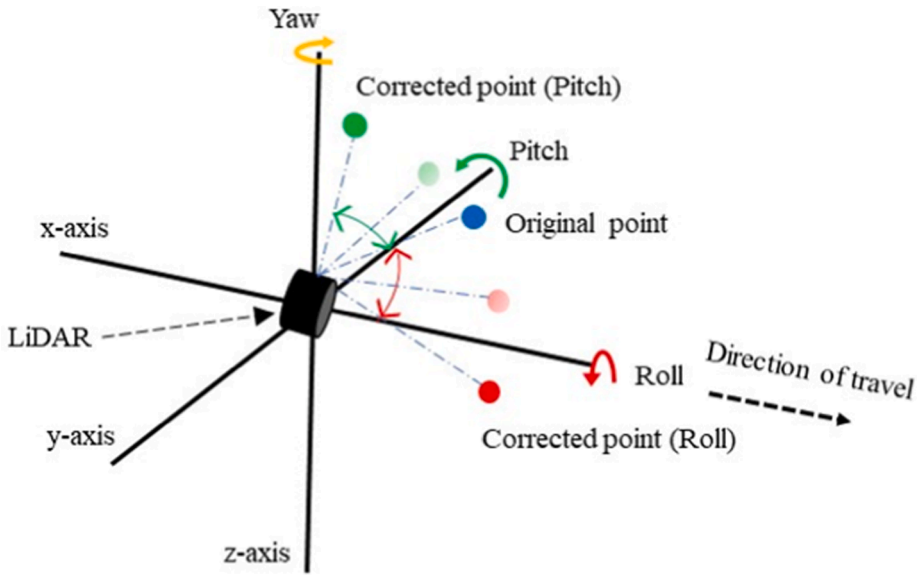

Fig. 2. An illustration of the roll, pitch, and yaw changes for point cloud position correction.

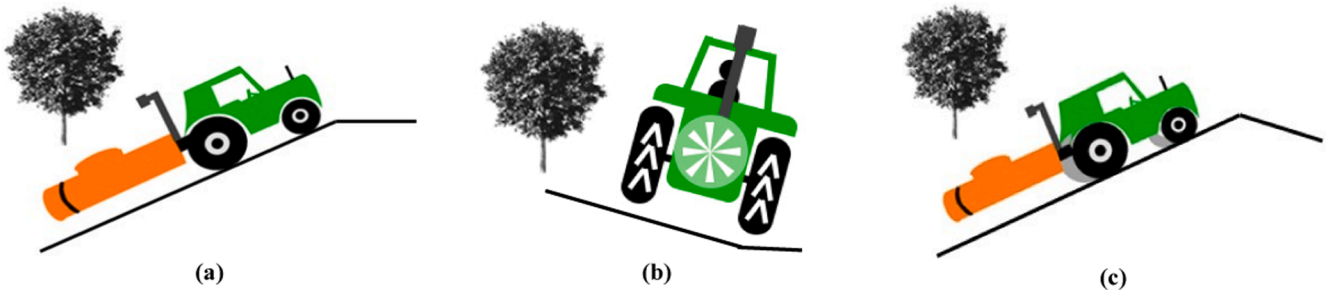

Fig. 3. Three different types of slopes in the apple orchard (a) longitudinal slope, (b) lateral slope, and (c) combination of both longitudinal and lateral slopes.

data scans. The LiDAR sensor was installed on an aluminum frame with a height of 1.70 m above the soil ground.

The LiDAR sensor consisted of sixteen vertically separated laser beams with a range of 30° (+15° to −15° up and down) and an angular resolution of 2°. The sensor could scan up to 0.3 million points per second. For the GNSS system, a base/reference station was set up to calculate the integrated system position based on satellite signals and compared the location to the known reference location. The difference was utilized to correct the GNSS data recorded by the rover (positioned at utility vehicle). A graphical illustration of connection for real-time kinematic (RTK) solution receiving by using an STRSVR tool is shown in Fig. 5. The base antenna was set up on a tripod positioned in an unobstructed location with a clear view of the sky. The base station was connected to the host computer, and a serial terminal program (RealTerm) was used for the device configuration. A streaming server (STRSRV tool) was used to translate the data coming from the base station. To transmit the correction data from the base station, an NTRIP (Network Transport for RTCM via Internet Protocol) server was set up on the host computer. The data were received using the computer connected to the rover (called rover computer). The STRSRV tool was utilized again to translate the data received by the rover computer. A GNSS-reader (Inertial Labs, Paeonian Springs, VA, USA) was used for the raw GPS data recording from the receiver. The INS-GNSS unit was connected to the rover computer through universal serial bias (USB).

Fig. 4. Integrated hardware system for canopy position corrections.

The unit consisted of an inertial measurement unit and a georeferenced positioning unit. The INS-GNSS sensor was mounted on the same aluminum frame where the LiDAR was installed to observe the positioning error of scanned point cloud data. Two antennas were installed on the roof of the utility vehicle (primary at the back; secondary at the front). The primary antenna was mounted with a vertical-up distance of 0.17 m and a forward distance of 1.16 m from the INS-GNSS sensor, and the corresponding distances were 0.22 and 2.15 m for the secondary antenna. The antennas were connected to the INS-GNSS sensor through cables. Both antennas were installed parallel to the INS unit where alpha (0°) and beta (2.94°) angles of the antennas baseline orientation were relative to the INS unit. The alpha angle was measured in the horizon plane of the carrier object (utility vehicle) with a clockwise direction as positive. The beta angle was measured in the vertical plane with an upward direction as positive. A graphical user interface (INS_GUI) (Inertial Labs, Paeonian Springs, VA, USA) was used to visualize and record the acquired data from the INS-GNSS unit. Raw IMU data was created from pair files (BIN and PRM) with extensions (.bin and .prm), which

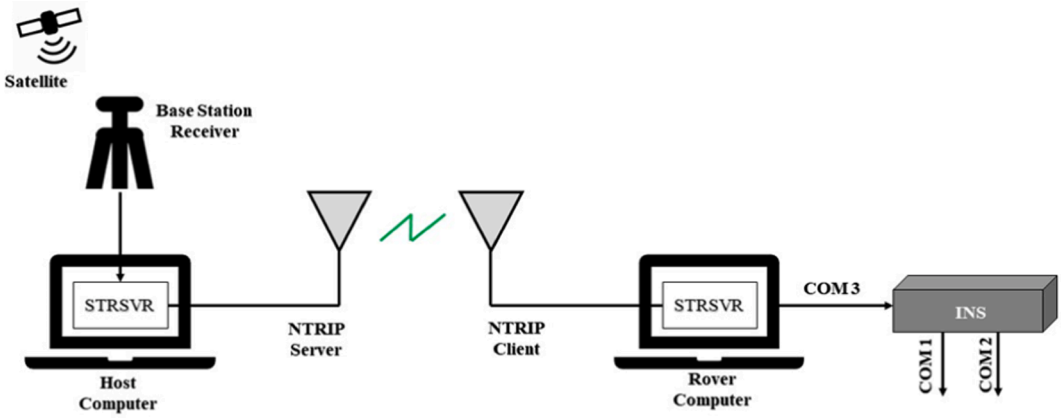

Fig. 5. Connection for real-time kinematic (RTK) solution receiving by using STRSVR tool.

were saved during the experiments.

2.3. Test orchards

To evaluate the developed sensor system, three orchard sites with different terrain conditions were selected. The orchard sites were: site 1: Gala variety (39°56′20.4″N 77°15′24.3″W), site 2: Golden Delicious variety (39°56′24.8″N 77°15′26.1″W), and site 3: Gala variety (39°56′20.0″N 77°15′24.8″W), located at the Penn State Fruit Research and Extension Center (FREC), Biglerville, PA, USA. Trellis system was used in all orchard sites to support trees trained with a tall spindle structure. The tree-to-tree spacings were 1.22, 1.40, and 1.22 m for orchard sites 1, 2, and 3, respectively. The average tree height and width was 3.5 m and 1.20 m for all three orchard sites. At all orchard sites trees had dense canopy foliage. Trees were tied with three tiers of trellis wires and support poles. Three slopes, including longitudinal, lateral, and combination of both (longitudinal and lateral slopes), were studied from orchard sites 1, 2, and 3, respectively. The slopes were distinct at different places among the apple tree rows. A single apple tree row from each orchard site was used for the study.

2.4. Sensor data acquisition

The integrated LiDAR and INS-GNSS systems were used to acquire tree canopy foliage data from three orchard sites. The data acquisition was performed while driving through the orchard tree row. The utility vehicle speed was about 4.5 km.h^{-1} (±0.5) during data scans. The data were collected from the center of the tree row in each orchard site.

A LiDAR data acquisition algorithm was scripted in MATLAB® software. To receive data from the LiDAR (VLP-16) sensor, the *velodynelidar()* function was used to create a 3D object. The MATLAB uses a default UDP port value of 2368 to receive point cloud data from the sensor. The frame size in x, y, and z-axis directions was defined (default frame size used) before data scans. The *start()* function was used to start the data acquisition. Both the frames and timestamps were saved in the computer for processing. Timestamp was stored in milliseconds. The timestamp was important to conduct the fusion between LiDAR and INS-GNSS unit data. The Euler angles (roll, pitch, and yaw) and georeferenced location (longitude, latitude, and altitude) were acquired from the INS-GNSS unit. The INS-GNSS provided data at every twenty milliseconds. The acquired data from LiDAR and INS-GNSS unit was fused, followed by the correction of the canopy point position in the processing section.

2.5. Data processing for canopy position corrections

Processing algorithms were developed to process the tree canopy point corrections considering different sloping conditions with the acquired data from the LiDAR and INS-GNSS units. Data processing steps include pre-processing, sensor fusion algorithm development, and canopy corrections.

2.5.1. Point cloud data pre-processing

The MATLAB® software was used to pre-process the acquired 3D-

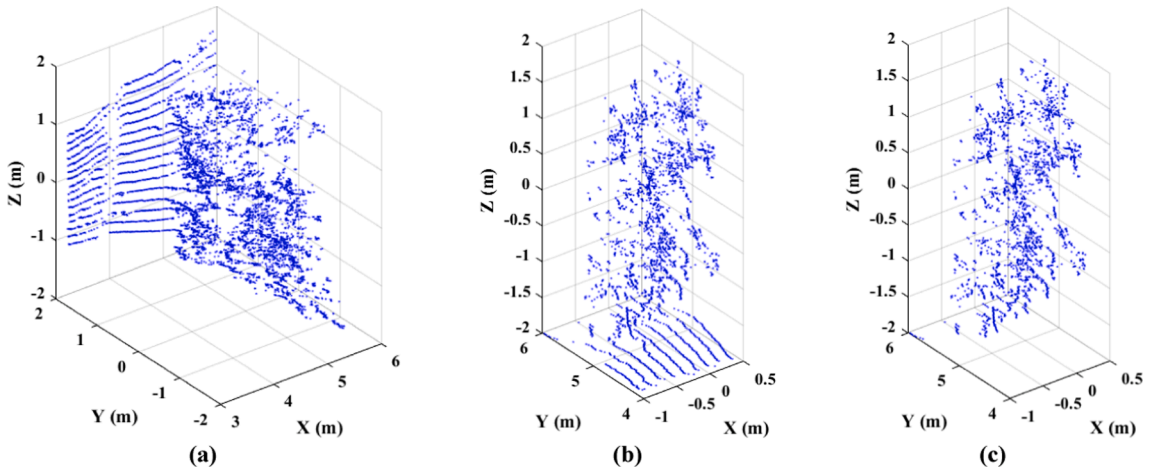

Fig. 6. Point cloud data pre-processing using MATLAB® software (a) raw point cloud data (b) transformed point cloud data (c) segmented tree point cloud of an apple tree.

point cloud data from the tree canopies. The raw scanned point cloud data was read by using a Velodyne file reader function (*velodyneFileReader*). An individual tree was selected for point cloud data-position correction. Since the frame rate of the LiDAR was five per second, it captured multiple frames from a single tree. Some of the frames included points from two consecutive trees, and some were overlapped. Therefore, it was important to find the frame that only includes the selected tree for canopy position correction. Point cloud data from the targeted tree was localized with the origin point (located at the center of the sensor). A coordinate system was specified where the x-axis was along the tree row, the y-axis was perpendicular to the tree row along the horizontal plane, and the z-axis was vertically upward along the tree trunk. The acquired point cloud data were positioned at 90° counterclockwise due to the setup of the LiDAR sensor (Fig. 6a). The rotation of the point cloud data was performed at 90° counterclockwise around the z-axis and then 90° clockwise around the y-axis to make the tree straight as the original tree position. The acquired point clouds also included the points from different trees in different rows, ground vegetation, and other objects sited in the orchards. Targeted points from the selected tree were extracted by setting a region of interest (ROI). The ROI was different among the three orchard sites due to the position of the LiDAR relative to the trees. The ROI of −1.0 to 0.5 m in the x-axis, 4 to 6 m in the y-axis, and −2 to 2 m in the z-axis were selected in orchard site 1. The ROI of −1.0 to 0.0 m in the x-axis, 2 to 4 m in the y-axis, and −2 to 2 m in the z-axis were used for orchard site 2. The ROI of −0.5 to 1.0 m in the x-axis, −3.75 to −1.75 m in the y-axis, and −2 to 2 m in the z-axis was applied for orchard site 3.

To remove the ground vegetation points at the bottom of the tree (Fig. 6b), a *pcfitplane()* function was used to fit the plane in the 3D point cloud. This function uses the M-estimator SAmple Consensus (MSAC) algorithm to find a plane. The best plane among the 3D point clouds was identified using the MSAC algorithm, which is a variant of RANSAC algorithm (Torr & Zisserman, 2000). A maximum distance of 0.15 m and the reference vector to the z-axis the direction was utilized to the plane fitting for ground segmentation. The MSAC algorithm was used to find the outlier points from the point cloud data. The outliers were removed to eliminating the ground vegetation points from the input data (Fig. 6c). Tree canopy point cloud data (without the ground vegetation points) along with timestamp were saved in a MATLAB file for processing.

2.5.2. IMU and GNSS data pre-processing

Raw IMU and GNSS data were stored in the BIN file (.bin) from the INS-GNSS graphical user interface (GUI), which was not suitable to use in the processing algorithm. The BIN file was converted to the text file (.csv) using the convert function from the GUI. The text file was then

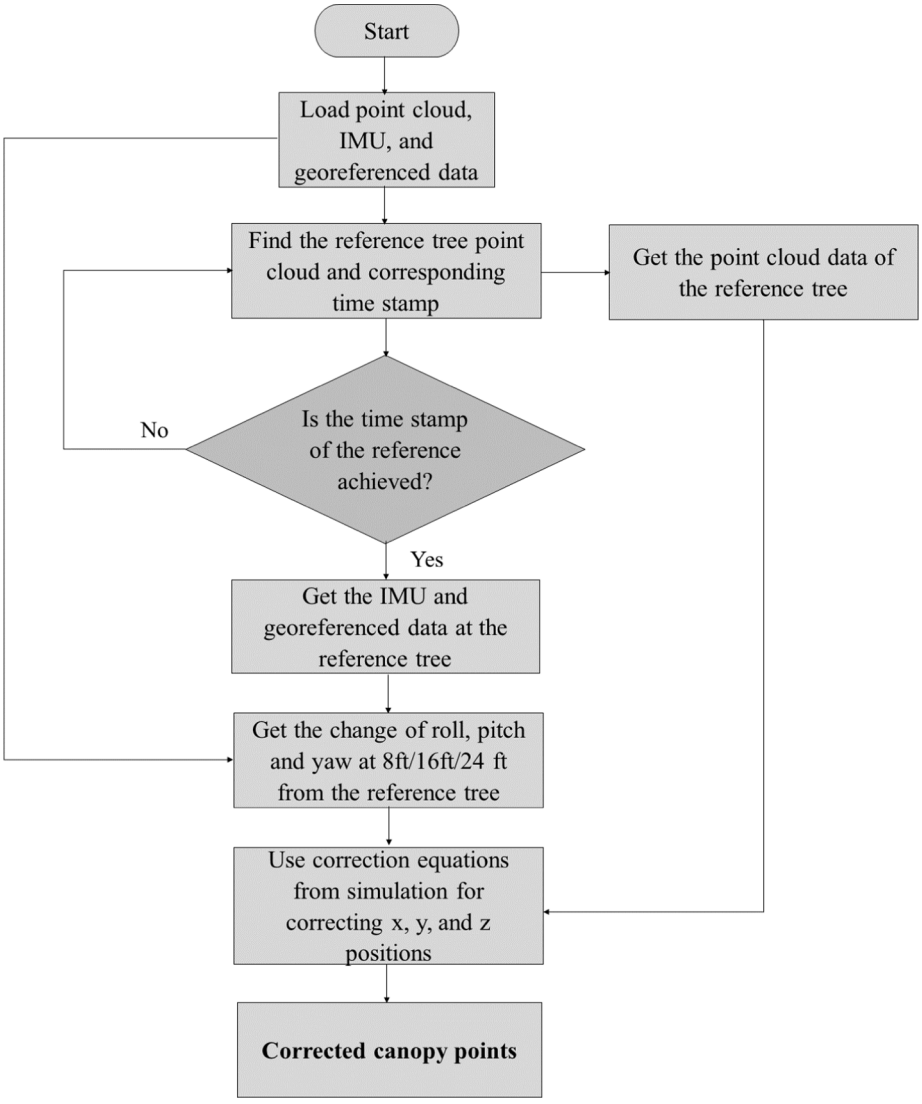

Fig. 7. Sensor fusion algorithm for canopy point corrections (the roll, pitch and yaw angles were collected based on soil ground slope in three orchard sites).

converted to the MATLAB file where the roll, pitch, and yaw values and georeferenced position (longitude, latitude, and altitude) were stored with the corresponding timestamp. The stored data were utilized for the sensor fusion algorithm.

2.5.3. Sensor fusion algorithm for canopy point corrections

To correct the tree canopy points, a sensor fusion algorithm was developed in MATLAB® software with the pre-processed sensor data. (Fig. 7). The algorithm began with loading the pre-processed LiDAR and INS-GNSS data. The LiDAR data included the canopy point clouds, and the INS-GNSS data contained the roll, pitch, and yaw, and georeferenced location of the tree. For each orchard site, the reference tree point cloud frame was extracted and considered as faulty/incorrect tree canopy data. The corresponding timestamp of the reference tree point cloud acquisition was obtained. After obtaining the timestamp of the reference tree, the roll, pitch, and yaw, and the georeferenced location of the tree were extracted. With different sprayer sizes, the distance between the LiDAR sensor and nozzles could be different. Three distances of 2.44 m (8 ft), 4.88 m (16 ft), and 7.32 m (24 ft) were chosen in this study, considering three different distances/positions between sensor and nozzles. The timestamps were obtained at three distances from the reference tree position for orchard site 1 (site with longitudinal slope), orchard site 2 (site with lateral slope) and 3 (site with both longitudinal and lateral slopes). Three timestamps were selected based on the utility vehicle speed (4.5 km.h^{-1}), where the algorithm extracted the times as 1 s and 940 ms, 3 s and 900 ms, and 5 s and 860 ms for terrain evaluation at 2.44, 4.88, and 7.32 m, respectively. The roll, pitch, and yaw were extracted at three different times. Subtraction was performed between the roll, pitch, and yaw acquired at 2.44, 4.88, and 7.32 m from the initial roll, pitch, and yaw at the reference tree position to find the variation of the slope (changes of the roll, pitch, and yaw). The differences of the roll, pitch, and yaw were used in the mathematical model (equations derived in section 2.1) for the correction of the tree canopy points.

2.6. Canopy density and off-target deposition

The canopy density of a tree is defined as canopy points per grid area. After correcting canopy points from individual trees, the tree canopy density was calculated for the canopies before and after correction. Individual trees were divided into small grid areas with an equal size of 29 cm^2. The canopy density map of each individual tree was generated using the canopy points that were scanned from the respective tree grids. The canopy density map was generated using the algorithm developed by He (2020).

2D boundaries at xz plane for both the scanned and corrected canopies were created to visualize and calculate the difference of the boundary areas while facing the individual trees. The area changes between the two 2D boundaries were calculated to examine the change of tree shape in the x-axis and z-axis direction. The intersection of the two boundaries from scanned and corrected canopies was determined. The area of the scanned canopies and intersectional boundaries was calculated. The subtraction between two calculated areas was performed to measure the possible off-target region or depositional area due to the slope change in the orchards. The percentage of probable off-target deposition of individual tree was calculated by the ratio of the off-target region and original scanned tree canopy area.

3. Results and discussion

3.1. Simulation results for changes in roll, pitch, and yaw

Table 1 shows the simulation results for the canopy point corrections with respect to the 20° change of both the roll and pitch angles. More results due to independent roll and pitch change are presented in the Figure A as supplementary material. Twenty canopy points from an apple tree and their corresponding corrections are illustrated. With the change of 20° for both roll and pitch, the average canopy position was changed to about 0.56 m in the x-axis, 0.35 m in the y-axis, and 1.18 m in the z-axis directions. Results showed that the position change in the z-axis was greater compared to the x and y-axis directions. When the roll changes, the position change of these points occurred in the y and z-axis directions, and when the pitch changes, the position change of these points occurred in the x and z-axis direction (Table 1). In the simulation, the yaw angle was not considered because when the sprayer was traveling straight through the orchard row, the angle change around the z-axis (yaw angle) was negligible. The possibility of yaw angle change is relatively low compared to the roll and pitch angle. The change in roll or pitch angle could influence the magnitude and orientation of the canopy point position movement/correction. For example, when the roll angle of the sprayer is 0°, and if the sprayer moves uphill, there will be no position change along the x-axis. However, if the roll angle is not zero, with the sprayer moving uphill, the position change can occur in the x, y, and z-axis. Similarly, if the pitch angle of the sprayer is 0°, the roll

Table 1
Simulation results for tree canopy point corrections.

Acquired Canopy Point Cloud Data (m)			Corrected Canopy Point Cloud Data[a] (m)		
X-axis	Y-axis	Z-axis	X-axis	Y-axis	Z-axis
−0.3741389	2.4954416	−1.74862551	−0.949640696	2.863179554	−0.570337959
−0.3719452	2.4838406	−1.73404051	−0.942590976	2.847847258	−0.562131877
−0.3738951	2.4999006	−1.73877065	−0.946041097	2.864230844	−0.560189176
−0.3724327	2.4931417	−1.7276210	−0.940853456	2.854467195	−0.553125488
−0.3724327	2.4961532	−1.72326702	−0.939364306	2.855897707	−0.548250842
−0.3741389	2.5106061	−1.72678237	−0.942169901	2.870409201	−0.545863441
−0.3751138	2.5201662	−1.72688624	−0.943121585	2.879312109	−0.542372064
−0.3758451	2.5280948	−1.72584276	−0.943451814	2.886341669	−0.538503896
−0.3763325	2.5343860	−1.7236605	−0.943163514	2.891495069	−0.534268521
−0.3785262	2.5521810	−1.72925598	−0.947138638	2.909758628	−0.53241819
−0.3821823	2.6039382	−1.70526788	−0.942369816	2.950257216	−0.492359104
−0.2731461	2.6115448	−1.71090064	−0.841835855	2.971970214	−0.529774896
−0.3753576	2.5603585	−1.67035055	−0.924014279	2.898881828	−0.478624863
−0.2721002	2.6045159	−1.6998065	−0.837058641	2.961922016	−0.522718668
−0.3743826	2.5566121	−1.66155238	−0.92008897	2.892647703	−0.472450584
−0.2722745	2.6091491	−1.69634419	−0.836038258	2.965142589	−0.518020714
−0.3746264	2.5611745	−1.65816655	−0.919159989	2.895818268	−0.467822054
−0.2703571	2.5937107	−1.67987378	−0.828603256	2.945566041	−0.509373477
−0.3746264	2.5640646	−1.65369394	−0.917630265	2.897096644	−0.462884147
−0.2682654	2.5765486	−1.6623823	−0.820655227	2.924062007	−0.500470155

[a] Change of roll and pitch of about 20° (degree).

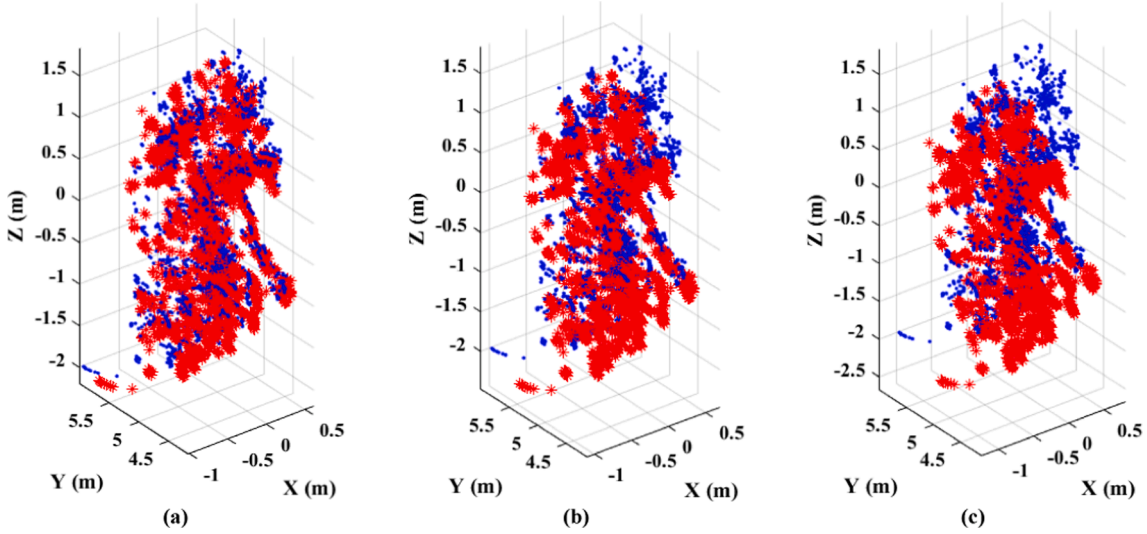

Fig. 8. Canopy point corrections in longitudinal slope; tree canopy point correction at three sensor-to-nozzle distances (a) 2.44 m (change of roll (1.29°), pitch (4.68°), and yaw (0.02°)) (b) 4.88 m (change of roll (3.36°), pitch (8.77°), and yaw (0.39°)), and (c) 7.32 m (change of roll (4.83°), pitch (13.46°), and yaw (0.57°)) from the reference tree (blue and red colors represent the tree canopy points before and after correction). (For interpretation of the references to color in this figure legend, the reader is referred to the web version of this article.)

rotation results in the position change along the x and z-axis. Although the simulation was performed based on 20° change of roll and pitch, it could be possible to correct the canopy position for any change in roll, pitch, and yaw by using the developed mathematical model. The developed model could be effectively utilized for almost every possible correction of the tree canopy points.

3.2. Field evaluation results

A single tree row was tested for canopy point correction from each orchard site. The correction was performed for all trees located in the orchard row, but the correction results of single tree canopies are presented from each orchard site as a reference.

3.2.1. Correction in orchard site 1

After point cloud data was acquired, each individual tree canopy could be corrected according to the sensor orientation at the tree location and the location when the sprayer nozzles (simulated) were passing the tree. Fig. 8 shows an example of a tree canopy correction in orchard site 1. Blue and red colors represent the tree canopy points before and after correction, respectively. The initial sensor orientation at the tree location was 2.32°, 12.04°, and 136.16° for the roll, pitch, and yaw, respectively. The corrections were made when the sensor was at the distances of 2.44, 4.88, and 7.32 m away from the reference tree, considering the sensor at the reference tree and distances are the assumed positions of the nozzles for three different sized sprayers. These distances are called sensor-to-nozzle distance. Since orchard site 1 was mainly in a longitudinal slope, the major change was noticed in the pitch angle. The pitch angle changes were 4.68°, 8.77°, and 13.46° for the

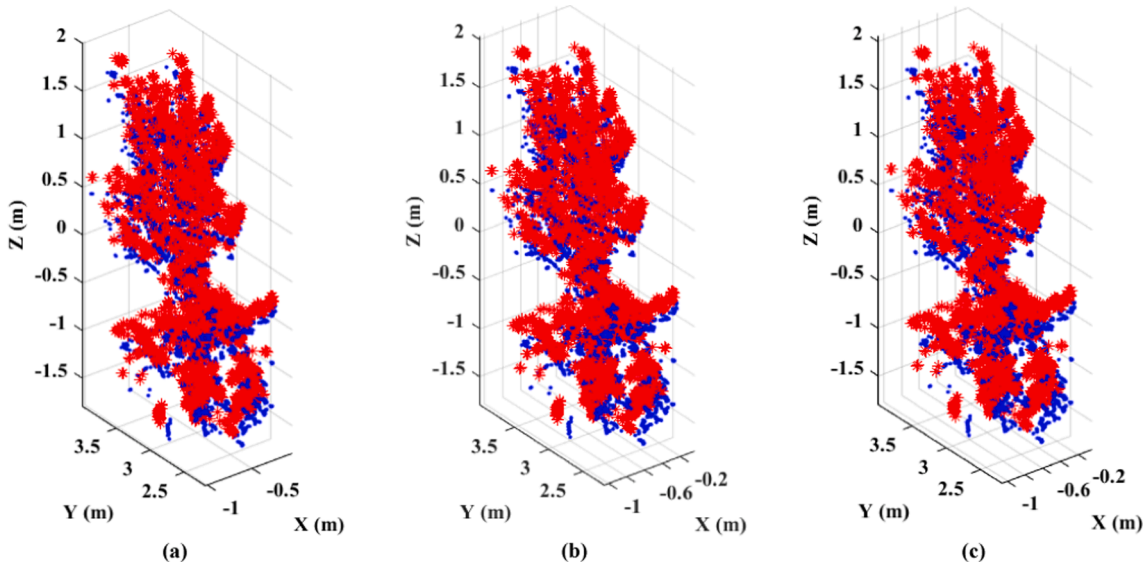

Fig. 9. Canopy point corrections in lateral slope; tree canopy point correction for side slope change at three sensor-to-nozzle distances (a) 2.44 m (change of roll (2.54°), pitch (1.28°), and yaw (0.39°)) (b) 4.88 m (change of roll (2.89°), pitch (1.94°), and yaw (0.61°)), and (c) 7.32 m (change of roll (3.15°), pitch (2.27°), and yaw (0.73°)) from the reference tree (blue and red colors represent the tree canopy points before and after correction). (For interpretation of the references to color in this figure legend, the reader is referred to the web version of this article.)

distance of 2.44, 4.88, and 7.32 m, respectively (assumed sensor-to-nozzle distances). The positive pitch angles were due to the subtraction from the uphill slope at 2.44, 4.88, and 7.32 m to the reference tree position. The highest pitch change was achieved at 7.32 m apart from the reference tree. The potential reason for the greatest pitch angle change at 7.32 m was the sharp change of the slope at that spot. Besides pitch angle, there were certain changes noticed in the roll angle (1.29°, 3.36°, and 4.83° at 2.44, 4.88, and 7.32 m apart from the reference tree, respectively) because of the side slope existence in the orchard site 1. The average movement of tree canopy points were 0.14, 0.24, and 0.37 m in the x-axis, 0.04, 0.12, and 0.18 m in the y-axis, and 0.15, 0.35, and 0.50 m in z-axis at 2.44, 4.88, and 7.32 m, respectively from the reference tree. The highest movement of tree canopy points in the x and z-axis direction was achieved at the pitch of 13.46°. The movement varied with the changes in the pitch angle, depending on the geometric components in the model equation (Eq. (2)). Among all axes, the highest movement was observed in the z-axis (0.50 m) at the position about 7.32 m apart from the reference tree, but the change in the pitch angle influences axis along which the largest change (x or z-axis) could occur. The geometric components in the rotational part of the model equation influenced the direction, and the geometric components in the position vector affected the magnitude of the movement along each axis.

3.2.2. Correction in orchard site 2

Correction in orchard site 2 was performed in the lateral slope, where the reference tree was located in the uphill direction (the roll, pitch, and yaw were 9.38°, 0.79°, and 135.38°, respectively), and the side slope was considered towards the downhill direction. Similar to orchard site 1, the corrections were performed at three sensor-to-nozzle distances: 2.44 (8 ft), 4.88 (16 ft), and 7.32 m (24 ft), and corrected canopy points were presented with red color (Fig. 9). For the reference tree, the major position change was noticed in the roll compared to pitch and yaw. The roll angle change was 2.54°, 2.89°, and 3.15° for side slope at 2.44, 4.88, and 7.32 m away from the reference tree position, respectively (Fig. 9). The highest roll angle of 3.15° was achieved at 7.32 m from the reference position due to the large change of the downhill slope compared to 2.44 m and 4.88 m. The average position change of tree canopy points was 0.04, 0.06, and 0.06 m in the x-axis, 0.02, 0.01, and 0.01 m in the y-axis, and 0.18, 0.22, and 0.23 m in z-axis at 2.44, 4.88, and 7.32 m, respectively (i.e., sensor-to-nozzle distances) from the reference tree. Although the system was tested at a lateral slope orchard, a certain amount of change was also noticed in the pitch angle as orchard site 2 had slight variations in terrain due to small uphill or downhill slope changes. The roll angle change indicated the great changes of the tree canopy points around the z-axis compared to the y-axis (Fig. 9), but the change of position around the axes (y and z) could vary, depending on the geometric components of the mathematical model. Considering the observation of this study, the lateral slope change (roll angle change) highly affected the canopy point position changes in the z-axis compared to the y-axis. However, it could be impacted differently (more changes in the y-axis) after a roll angle change, indicating no direct relationship. The magnitude of position changes due to the roll angle depended on the distance between the LiDAR sensor to the tree. That is, the magnitudes would increase if the distance increased. Based on trigonometry rules, for the same roll angle, the position change could be different, depending on the length of the base (distance between the LiDAR sensor to the tree in our case). For a larger sensor-tree distance, the position change would be greater and vice-versa. Even though the test was conducted in a lateral slope orchard, the variation of the slope was small. Therefore, no substantial changes were observed in the tree canopy position.

3.2.3. Correction in orchard site 3

Correction in combined two slopes (longitudinal and lateral) was processed for the apple trees planted uphill with two different slopes in the orchard site 3. Similar to the orchard site 1 and 2 tests, the evaluations were performed at three sensor-to-nozzle distances (i.e., 2.44, 4.88, and 7.32 m) considering the side slope from the reference tree (the roll, pitch, and yaw were 7.95°, 9.73°, and 136.55°, respectively) (Fig. 10).

Evaluation results suggested that the change in the utility vehicle movements appeared with both the roll and pitch angles. However, the change in pitch was greater among the Euler angles due to the sharp uphill slope, and the side slope was comparatively lower. The changes in the pitch angle were 7.95°, 10.24°, and 14.06° m for 2.44, 4.88, and 7.32 m, respectively. The values were 4.73°, 6.93°, and 8.79° for the change in the roll angle. The highest pitch angle of 14.06° and roll angle of 8.79° were noticed at 7.32 m away from the reference tree, where the slope changed suddenly. The average position change of tree canopy points was 0.24, 0.27, and 0.42 m in the x-axis, 0.16, 0.24, and 0.31 m in the y-axis, and 0.19, 0.30, and 0.34 m in z-axis at 2.44, 4.88, and 7.32 m, respectively from the reference tree. For the combined slopes, the tree

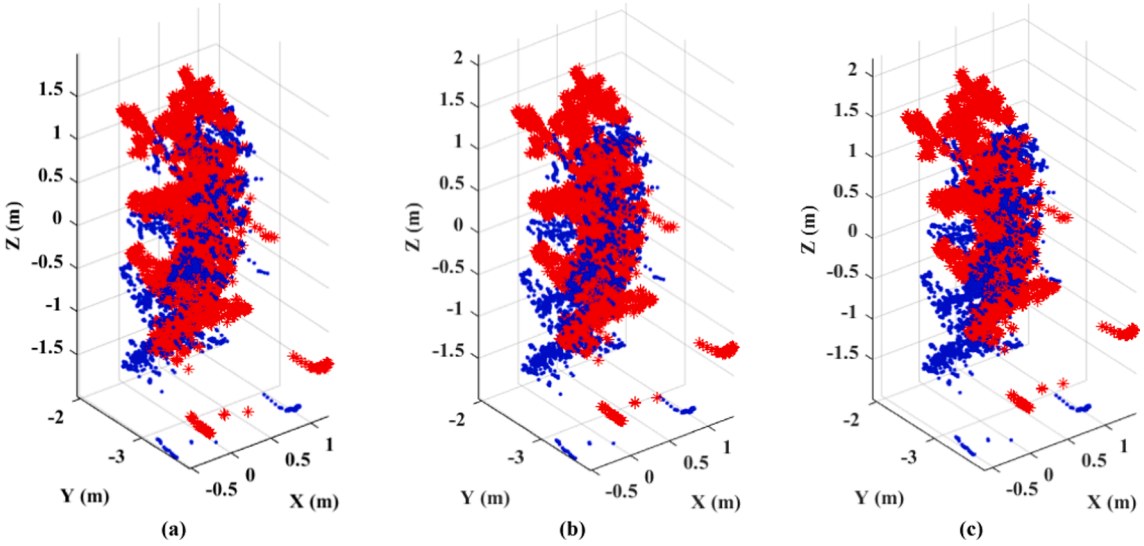

Fig. 10. Canopy point corrections in longitudinal slope; tree canopy point correction change at three sensor-to-nozzle distances (a) 2.44 m (change of roll (4.73°), pitch (7.95°), and yaw (0.41°)) (b) 4.88 m (change of roll (6.93°), pitch (10.24°), and yaw (1.22°), and (c) 7.32 m (change of roll (8.79°), pitch (14.06°), and yaw (0.71°)) from the reference tree (blue and red colors represent the tree canopy points before and after correction). (For interpretation of the references to color in this figure legend, the reader is referred to the web version of this article.)

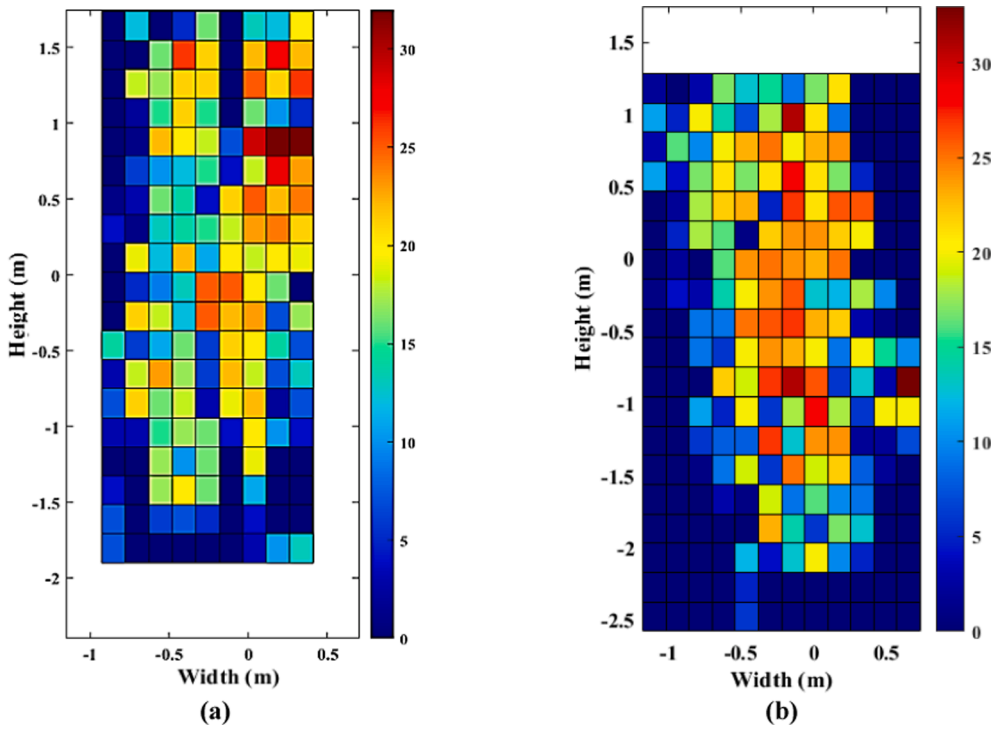

Fig. 11. Tree canopy density (canopy points per grid area) maps (a) before canopy points correction (b) after canopy points correction.

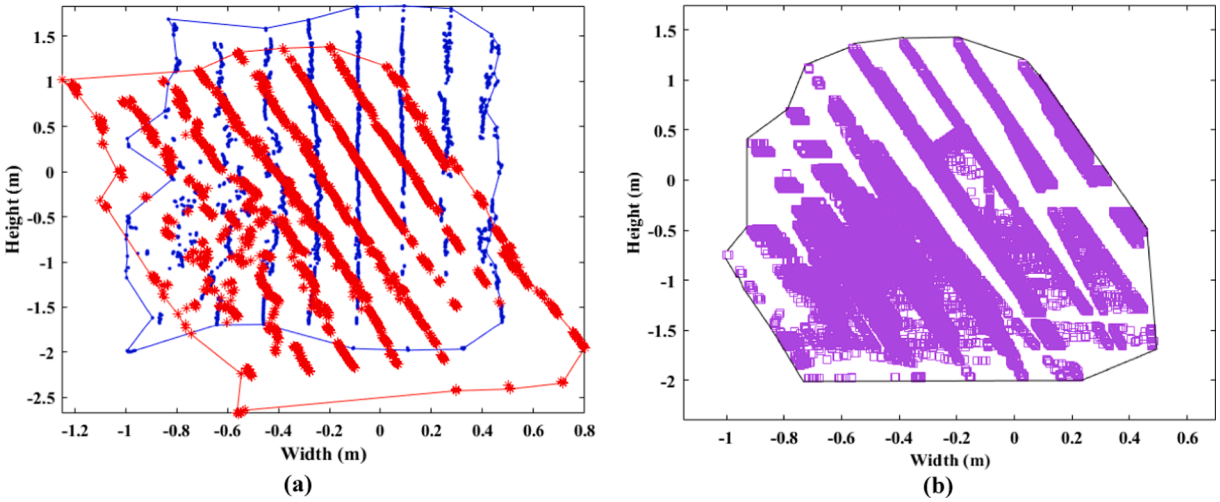

Fig. 12. Tree canopy points boundaries (a) canopy area displacement due to slope change (blue boundary: scanned canopies, red boundary: corrected canopies, (b) calculated intersection between two boundaries. (For interpretation of the references to color in this figure legend, the reader is referred to the web version of this article.)

canopy point position changes were noticed in all directions (x, y, and z-axis); however, the major movement was spotted in the x-axis (due to the pitch) and z-axis direction (due to the roll). The corrected canopy point moved up to the z-axis due to the change in the roll along with pitch angle. The greatest change was observed in the x-axis because of the maximum change in pitch angle.

3.3. Canopy density and calculation of Off-Target deposition

Tree canopy density maps were generated from scanned canopy points (before correction) (Fig. 11a, orchard site 1 as an example) and corrected canopy points (after correction) (Fig. 11b). The maps were produced based on the counted number of tree canopy points located at each grid. The canopies area from each tree (before and after correction) was divided based on fixed grid size in the x-axis and y-axis direction. The size of each grid was 0.15 m × 0.19 m (width × height) for scanned canopy and corrected canopy points. Due to the spread of the tree canopy points after correction, the number of grids was increased compared to the total number of scanned canopy points grids. The color bar on the right side shows the number of canopy points per grid area in the respective maps. Based on the canopy density maps, the width and height of the scanned tree before correction were 1.33 m and 3.6 m, respectively. After correcting canopy points, the width and height of the tree were changed to 1.85 m and 3.67 m, respectively, because of the slope change.

The boundary of the tree canopy points before and after corrections was created (Fig. 12a, orchard site 1 as an example). The blue boundary represents the area covered by the scanned canopy points (before

correction), and the red boundary shows the area of corrected canopy points. There was a displacement between the boundaries generated from the tree canopy points before and after corrections. The displacement area was provided information about the possible off-target deposition. To calculate the displacement area, the intersection between two boundaries was calculated (Fig. 12b). With the subtraction from the original tree area and intersectional area, the area of the possible off-target deposition was computed from individual trees. The field evaluation results indicated that the probable off-target deposition was up to 13.87% due to the slope changes in orchard site 1. With the same calculation, the corresponding off-target depositions were up to 5.19%, and 15.45% in the orchard site 2 and 3, respectively. These possible off-target depositions were calculated from the maximum slope changes in the respective orchard sites.

Tree canopy point correction is an important step towards accurate canopy characteristics measurements (e.g., tree height, width, canopy density and volume, etc.) as well as target-based spraying (precision spraying). Previous studies that utilized LiDAR-guided systems for tree canopy characterization highlighted the problem of positioning error while driving through the uneven terrain (Berk et al., 2020; Palleja et al., 2010; Underwood et al., 2016), but only a few studies have considered the corrected tree canopy points for the measurements. Although the developed canopy correction algorithm was tested in slopes with the highest roll, pitch, and yaw of 8.79°, 14.06°, and 1.22°, the system could be useful for correcting canopy position changes due to any type of slopes with changes in roll, pitch, and yaw in orchards. Even though there was no sprayer attached to the utility vehicle in the test, the study considered three sensor-to-nozzle distances (2.44, 4.88, and 7.32 m) for the evaluation of the system performance for longitudinal, lateral, and combined longitudinal and lateral slopes. Three distances were considered based on the assumed three different sizes of the precision sprayer. The major reason for considering three different distances was to correct the tree canopy points for any sized precision sprayer. Two common types of precision sprayers have become available for tree fruit orchards; one is a 3-point hitch mounted type, and the other one is pulled type (trailer type). The slope change between the mounted and pulled type precision sprayers will vary for the same length of sprayers. With the same length and size sprayer, the pulled type may have less position change due to the slope variation compared to the 3-point mount type sprayer. The developed correction algorithm could be used for the correction of the tree canopy points for any of these sprayers. However, installation of the INS-GNSS sensor should be accomplished at the position where the LiDAR sensor is installed. Distance between LiDAR sensor and INS-GNSS sensor may also affect the canopy point corrections in different terrain conditions, which will be evaluated in future studies. The canopy density map generated from the corrected tree canopy points visualizes the change of the tree shape and potential off-target depositional area due to the slope change. Although the maximum possible off-target deposition is calculated at about 15.45%, it could be higher if the variation of the slope increases. This study calculated the possible off-target deposition in the 2D surface rather than the 3D surface that should be sufficient to calculate accurate off-target deposition because the canopy points were corrected in the 3D space. When the canopy points change position in the y-axis, the depth of the canopy will change, but the shape of the tree will remain the same. Even y-axis changes were also included in the off-target deposition calculation because the canopy points used for the measurement were already corrected. The developed tree canopy correction system could be used to acquire accurate tree canopy points and density measurements, which will help reduce off-target spray deposition for precision spraying and save a substantial amount of agrochemicals for the apple growers.

To the best of our knowledge, this study is the first attempt for correcting apple tree canopy points to reduce off-target spray depositions due to slope changes. The study used a laptop computer throughout the experimental process. But the developed system can also be implemented with embedded systems, including Raspberry Pi or other small single-board computers. Our study integrated a LiDAR and an INS-GNSS system into a utility vehicle using the sensor fusion concept to gather canopy and orchard slope data. The sensor fusion concept combined two sources (LiDAR and INS-GNSS) of sensors data using the small timestamp to know about the tree canopies and corresponding slope variations of the canopy position to perform canopy correction and calculate possible off-target spray deposition. Although we processed the experimental data offline, the developed system has the capability of processing LiDAR data in real-time. However, we have relied on the timestamp for the INS-GNSS data process due to some limitations of the used sensor. Upon finding an alternative of the INS-GNSS system, which needs to have the capability of processing data on the onboard system. This system could be ready to use in real-time for tree canopy correction as well as reducing off-target spray deposition.

4. Conclusions

The positioning error of apple tree canopy points was corrected using a sensor fusion-based LiDAR-guided system. The sensor fusion algorithm was developed using 3D LiDAR and INS-GNSS sensors data through the corresponding timestamps. Mathematical model equations were developed to acquire the corrected position in the x, y, and z-axis with any roll, pitch, and yaw angle changes. The system was tested in three orchard sites planted at the longitudinal, lateral, and combination of longitudinal and lateral slopes, respectively. Tests were accomplished by assuming three different sized precision sprayers; therefore, the corrections were performed at three different sensor-to-nozzle distances. The data were scanned while driving the vehicle in the middle of the orchard drive rows, which is a common practice for spraying. The simulation was performed for evaluating the mathematical model performance for tree canopy point corrections. The simulation results suggested that the model could provide the corrected canopy point location for any change of roll, pitch, and yaw. Field evaluation results demonstrated that the system was able to correct the apple tree canopy points in different sloping conditions. Although the major movement was noticed in the z-axis for orchard sites 1 and 2 and in the x-axis for orchard site 3, the change of position was dependent on the geometric components in the model equation. The corrected canopy points were used to calculate accurate tree canopy density and possible off-target deposition measurements. The correction is needed for accurate tree canopy characteristics measurements when there is a slope change, with the goal of reducing off-target spray deposition. In the future, the integration of the state-of-art of this study will be merged with the precision sprayer for accurate tree canopy foliage density measurement aimed to reduce off-target chemical deposition due to slope change in tree fruit orchards. The nozzle flow rate of the precision sprayer will be regulated for applying variable-rate pesticides to the apple tree canopies.

CRediT authorship contribution statement

Md Sultan Mahmud: Conceptualization, Investigation, Methodology, Validation, Writing – original draft. **Azlan Zahid:** Methodology, Validation, Writing – review & editing. **Long He:** Conceptualization, Supervision, Writing – review & editing, Funding acquisition. **Daeun Choi:** Supervision, Writing – review & editing. **Grzegorz Krawczyk:** Supervision, Writing – review & editing. **Heping Zhu:** Supervision, Writing – review & editing.

Declaration of Competing Interest

The authors declare that they have no known competing financial interests or personal relationships that could have appeared to influence the work reported in this paper.

Acknowledgements

This study was supported in part by the United States Department of Agriculture (USDA)'s National Institute of Food and Agriculture (NIFA) Federal Appropriations under Project PEN04653 and Accession No. 1016510, a USDA NIFA Crop Protection and Pest Management Program (CPPM) competitive grant (Award No. 2019-70006-30440), and a Northeast Sustainable Agriculture Research and Education (SARE) Graduate Student Grant GNE20-234-34268. We would like to give special thanks to Dr. Phillip Martin for spending his time to review and improve this article.

Appendix A. Supplementary material

Supplementary data to this article can be found online at https://doi.org/10.1016/j.compag.2021.106565.

References

Asaei, H., Jafari, A., Loghavi, M., 2019. Site-specific orchard sprayer equipped with machine vision for chemical usage management. Comput. Electron. Agric. 162, 431–439.

Berk, P., Stajnko, D., Belsak, A., Hocevar, M., 2020. Digital evaluation of leaf area of an individual tree canopy in the apple orchard using the LiDAR measurement system. Comput. Electron. Agric. 169, 105158. https://doi.org/10.1016/j.compag.2019.105158.

Chakraborty, M., Khot, L.R., Sankaran, S., Jacoby, P.W., 2019. Evaluation of mobile 3D light detection and ranging based canopy mapping system for tree fruit crops. Comput. Electron. Agric. 158, 284–293.

Chen, L., Wallhead, M., Zhu, H., Fulcher, A., 2019. Control of insects and diseases with intelligent variable-rate sprayers in ornamental nurseries. J. Environ. Horticult. 37 (3), 90–100.

Chen, Y., Zhu, H., Ozkan, H.E., 2012. Development of a variable-rate sprayer with laser scanning sensor to synchronize spray outputs to tree structures. Trans. ASABE 55 (3), 773–781.

Gil, E., Escolà, A., Rosell, J.R., Planas, S., Val, L., 2007. Variable rate application of plant protection products in vineyard using ultrasonic sensors. Crop Prot. 26 (8), 1287–1297.

He, X., Zeng, A., Liu, Y., Song, J., 2011. Precision orchard sprayer based on automatically infrared target detecting and electrostatic spraying techniques. Int. J. Agric. Biol. Eng. 4 (1), 35–40.

He, C., 2020. densityplot(x,y,varargin) (https://www.mathworks.com/matlabcentral/fileexchange/65166-densityplot-x-y-varargin), MATLAB Central File Exchange. Retrieved on January 5, 2021.

Hosoi, F., Omasa, K., 2006. Voxel-based 3-D modeling of individual trees for estimating leaf area density using high-resolution portable scanning lidar. IEEE Trans. Geosci. Remote Sens. 44 (12), 3610–3618.

Hu, M., Whitty, M., 2019. An Evaluation of an Apple Canopy density mapping system for a variable-rate sprayer. IFAC-Papersonline 52 (30), 342–348.

Landers, A., 2011. Improving spray deposition and reducing drift - airflow adjustment is the answer. Retrieved from New York Fruit Quarterly 19 (4), 3–6. http://nyshs.org/wp-content/uploads/2016/10/1.Improving-Spray-Deposition-And-Reducing-Drift-—-Airflow-Adjustment-Is-The-Answer.pdf.

Landers, A.J., 2010. Effective vineyard spraying a practical guide for growers. Effective Spraying.

Liu, H., Zhu, H., 2016. Evaluation of a laser scanning sensor in detection of complex-shaped targets for variable-rate sprayer development. Trans. ASABE 59 (5), 1181–1192.

Miranda-Fuentes, A., Rodríguez-Lizana, A., Gil, E., Agüera-Vega, J., Gil-Ribes, J.A., 2015. Influence of liquid-volume and airflow rates on spray application quality and homogeneity in super-intensive olive tree canopies. Sci. Total Environ. 537, 250–259.

Omasa, K., Hosoi, F., Konishi, A., 2007. 3D lidar imaging for detecting and understanding plant responses and canopy structure. J. Exp. Bot. 58 (4), 881–898.

Palleja, T., Tresanchez, M., Teixido, M., Sanz, R., Rosell, J.R., Palacin, J., 2010. Sensitivity of tree volume measurement to trajectory errors from a terrestrial LIDAR scanner. Agric. For. Meteorol. 150 (11), 1420–1427.

Pimentel, D., Burgess, M., 2014. Environmental and economic costs of the application of pesticides primarily in the United States. Integr. Pest Manage. 3, 47–71.

Shalal, N., Low, T., McCarthy, C., Hancock, N., 2015. Orchard mapping and mobile robot localisation using onboard camera and laser scanner data fusion - Part A: tree detection. Comput. Electron. Agric. 119, 254–266.

Song, Y., Sun, H., Li, M., Zhang, Q., 2015. Technology application of smart spray in agriculture: a review. Intell. Autom. Soft Comput. 21 (3), 319–333.

Torr, P.H.S., Zisserman, A., 2000. MLESAC: A new robust estimator with application to estimating image geometry. Comput. Vis. Image Underst. 78 (1), 138–156.

Underwood, J.P., Hung, C., Whelan, B., Sukkarieh, S., 2016. Mapping almond orchard canopy volume, flowers, fruit and yield using lidar and vision sensors. Comput. Electron. Agric. 130, 83–96.

Zeng, L., Feng, J., He, L., 2020. Semantic segmentation of sparse 3D point cloud based on geometrical features for trellis-structured apple orchard. Biosyst. Eng. 196, 46–55.

Zhang, Z., Wang, X., Lai, Q., Zhang, Z., 2018. Review of variable-rate sprayer applications based on real- time sensor technologies. In: Automation in Agriculture - Securing Food Supplies for Future Generations.